




Jastrow wave function for the spin-1 Heisenberg chain: The string order revealed by the mapping to the classical Coulomb gas

Davide Piccioni ^{1,*} Christian Apostoli ² Federico Becca³ Guglielmo Mazzola⁴ Alberto Parola ⁵ Sandro Sorella,¹ and Giuseppe E. Santoro^{1,6,7}

¹*Scuola Internazionale Superiore di Studi Avanzati (SISSA), Via Bonomea 265, I-34136 Trieste, Italy*

²*Dipartimento di Fisica “Aldo Pontremoli”, Università degli Studi di Milano, via Celoria 16, I-20133 Milano, Italy*

³*Dipartimento di Fisica, Università di Trieste, Strada Costiera 11, I-34151 Trieste, Italy*

⁴*Institute for Computational Science, University of Zurich, Winterthurerstrasse 190, 8057 Zurich, Switzerland*

⁵*Dipartimento di Scienza e Alta Tecnologia, Università dell’Insubria, Via Valleggio 11, I-22100 Como, Italy*

⁶*International Centre for Theoretical Physics (ICTP), Strada Costiera 11, I-34151 Trieste, Italy*

⁷*CNR-IOM, Consiglio Nazionale delle Ricerche—Istituto Officina dei Materiali, c/o SISSA, Via Bonomea 265, I-34136 Trieste, Italy*



(Received 31 May 2023; accepted 11 September 2023; published 21 September 2023)

We show that a two-body Jastrow wave function is able to capture the ground-state properties of the $S = 1$ Heisenberg chain with nearest-neighbor superexchange J and single-ion anisotropy term D , in both the topological and large- D phases (with $D/J \geq 0$). Here, the optimized Jastrow pseudopotential assumes a very simple form in Fourier space, i.e., $v_q \approx 1/q^2$, which is able to give rise to a finite string-order parameter in the topological regime. The results are analyzed by using an exact mapping from the quantum expectation values over the variational state to the classical partition function of the one-dimensional Coulomb gas of particles with charge $q = \pm 1$. Here, two phases are present at low temperatures: the first one is a diluted gas of dipoles (bound neutral pairs of particles), which are randomly oriented (describing the large- D phase); the other one is a dense liquid of dipoles, which are aligned thanks to the residual dipole-dipole interactions (describing the topological phase, with the finite string order being related to the dipole alignment). Our results provide an insightful interpretation of the ground-state nature of the spin-1 antiferromagnetic Heisenberg model.

DOI: [10.1103/PhysRevB.108.104417](https://doi.org/10.1103/PhysRevB.108.104417)

I. INTRODUCTION

Since the early days of quantum mechanics, the simulation of correlated quantum many-body systems has been an interesting problem in physics. Due to the paucity of exact results, many different approximation schemes have been proposed, most of them relying on some kind of variational *Ansatz*, including the variational quantum Monte Carlo approach, where the square modulus of a trial wave function is sampled by a Markov chain Monte Carlo algorithm [1]. In the last few years, many efforts have been devoted to improving the variational description of correlated quantum many-body system by various approaches, including tensor networks [2–4] and machine-learning techniques *Ansätze* [5,6]. However, these powerful approaches feature a large number of parameters, which may be difficult to optimize, and do not offer a transparent physical interpretation. By contrast, the Jastrow wave function [7] was introduced in 1955 to describe strongly correlated systems on the continuum and found one of its first and most important applications in the description of the ground state of ^4He [8]. The Jastrow state is a simple variational *Ansatz*, including a correlation operator acting on an uncorrelated state, hence allowing for a clear physical interpretation of its parameters after the optimization. In its

simplest definition (as used in the early applications [8]), the correlation factor involves two-body terms.

While it is obvious that modern *Ansätze* can provide quantitatively better results compared to Jastrow states on several microscopic systems (e.g., $S = 1/2$ Heisenberg models [5]), it would be interesting to identify cases where these sophisticated trial states outperform qualitatively the simple Jastrow wave functions, i.e., where the application of a more accurate *Ansatz* predicts the emergence of unconventional phases of matter. For example, accurate machine-learning inspired *Ansätze* have successfully improved the energy of benchmark problems with known solutions, but only rarely provided additional understanding on contested phase diagrams. To provide physical insights on the ground-state properties of correlated models, they are often combined with more traditional approaches, like in the case of frustrated spin models in two and three dimensions, most notably the $J_1 - J_2$ model on the square lattice [9] and the Heisenberg model on the pyrochlore lattice [10].

The quantum $S = 1$ antiferromagnetic Heisenberg chain, including the single-ion anisotropy term, provides a fair example of a simple model that displays a rich phenomenology. The Hamiltonian is given by

$$\hat{\mathcal{H}} = J \sum_{j=1}^L \hat{\mathbf{S}}_j \cdot \hat{\mathbf{S}}_{j+1} + D \sum_{j=1}^L (\hat{S}_j^z)^2, \quad (1)$$

*dpiccioni@sissa.it

where $\hat{S}_j = (\hat{S}_j^x, \hat{S}_j^y, \hat{S}_j^z)$ is the spin-1 operator on the j th site and periodic boundary conditions are assumed on chains with L sites. The interest in the model with $D = 0$ grew after Haldane proposed his conjecture about integer-spin chains being gapped [11]. Later, an exact solution was found by Affleck-Kennedy-Lieb-Tasaki (AKLT) for the case where a biquadratic interaction is added [12], the ground state being gapped and unique with periodic boundary conditions, featuring exponentially decaying correlations, as predicted by Haldane for the Hamiltonian of Eq. (1) with $D = 0$. Furthermore, the existence of a hidden $Z_2 \times Z_2$ symmetry has been highlighted [13], which is broken in this gapped ground state. More recently, the Haldane state has been recognized as an example of a symmetry-protected topological phase [14], with exponentially decaying spin-spin correlation functions and a nonlocal order parameter that is revealed by the so-called string operator [13,15]:

$$\hat{O}_{i,j}^{\text{string}} \equiv \hat{S}_i^z \exp \left\{ i\pi \sum_{l=i+1}^{j-1} \hat{S}_l^z \right\} \hat{S}_j^z. \quad (2)$$

The nonlocal order corresponds to a finite average value $C_{i,j}^{\text{string}} \equiv \langle \hat{O}_{i,j}^{\text{string}} \rangle$, computed on the ground state, at large distance:

$$\lim_{|i-j| \rightarrow \infty} C_{i,j}^{\text{string}} \neq 0. \quad (3)$$

The ground-state properties of the Hamiltonian of Eq. (1) have been investigated using a large variety of numerical techniques, including exact diagonalizations [16], density-matrix renormalization group (DMRG) approaches [17,18], and stochastic-series expansion techniques [19,20]. In addition, a variational Monte Carlo approach based on Gutzwiller-projected wave functions in the fermionic representation has been employed, showing a high accuracy in describing the ground state of $S = 1$ Heisenberg model [21]. Besides the Haldane phase, there are two other phases that are stabilized for large negative and positive values of D/J (with $J > 0$): the first one is a (doubly degenerate) Néel antiferromagnet that can be adiabatically connected to the Ising configuration where all spins align along the z axis, i.e., on each site the z component of the spin operator assumes values $m_j = \pm 1$; the second one is a spin-nematic phase, where the ground state is connected to a state in which the z component of the spin vanishes on each site, i.e., $m_j = 0$. The transition between the Haldane and the nematic phases is particularly interesting because it has a topological character, with a gapless critical point, which has been recognized to be a gapless Tomonaga-Luttinger liquid phase [20].

In this paper, we show that, despite its apparent simplicity, a Jastrow wave function is able to give a qualitatively correct description of the ground state of the $S = 1$ Heisenberg antiferromagnetic chain, including the Haldane phase. In the following, we will focus on the case with $D/J \geq 0$. Our research is motivated by the fact that, in the context of the one-band Hubbard model, it has been shown that an appropriate Jastrow factor is able to turn a gapless metal or superfluid into a gapped Mott insulator [22,23]. We also mention that a Jastrow wave function for generalized AKLT models has been proposed [24], exploiting the analogy between the

valence-bond states (within the Schwinger-boson representation) and the Laughlin wave function for the fractional quantum Hall effect [25]. Within spin models, the Jastrow Ansatz has been largely employed, mainly for $S = 1/2$ cases [26]. However, it appears rather nontrivial that a Jastrow wave function is able to represent a state with a finite string-order parameter. The issue is that the Jastrow wave function is parametrized by a two-body pseudopotential v_r that describes the spin-spin correlations at distance r and, therefore, it is not obvious that it is able to capture many-body correlations, like the string correlation that includes the knowledge of *all* spin values between two (distant) sites. Instead, we show that it is actually possible to properly represent the Haldane phase, the string correlations arising thanks to the long-range character of the pseudopotential v_r , i.e., $v_q \approx 1/q^2$ in Fourier space.

Remarkably, the fully optimized v_r can be well approximated by using only two parameters, one regulating the density of nonzero m_j and the other one defining the strength of correlations between (distant) pairs of spins, i.e., m_j and m_{j+r} . Most importantly, assuming this simplified version of the pseudopotential, we perform a mapping between the modulus squared of the Jastrow factor and the partition function of a *one-dimensional* classical Coulomb gas. Then, the properties of the variational state are related to (thermal) ones of the corresponding classical model. The use of similar mappings has proved to be very useful in strongly correlated systems, the most notable example is given by the Laughlin state for the fractional quantum Hall effect [25]. On the lattice, a similar approach has been used for the density-density Jastrow factor to investigate the resulting metal-insulator (Mott) transition [27]. In the present context, the classical model is a Coulomb gas of particles with charge $q = \pm 1$. Here, two phases are present at low temperatures (relevant for the actual pseudopotential). The first one is described by a diluted gas of dipoles with $m_j = \pm 1$, on top of a background with $m_j = 0$; these dipoles are randomly oriented, since thermal fluctuations overcome the residual dipole-dipole interaction. This phase corresponds to the nematic phase with large values of D/J . The second one contains a dense liquid of dipoles, which are aligned (hence, ordered) in space. Here, a finite string order is present, leading to a correct description of the Haldane phase for small values of D/J . The transition between these two phases is first order at low temperatures, with a jump in the charge density and a string-order parameter that also jumps from zero to a finite value; instead, at larger temperatures, the transition changes nature, with no discontinuity in the charge density and a string-order parameter that varies continuously from zero to a finite value.

The results obtained by using the simplified version of the pseudopotential give an insightful vision of the ground-state nature of the $S = 1$ Heisenberg model. However, on finite clusters, close to the transition between the topological and large- D phases, there is a small region where the functional form of v_r deviates from its simplified version, showing a less singular behavior at small- q values $v_q \approx 1/q$. Here, robust spin-spin correlations are present in the x - y plane, suggesting the existence of long-range order and gapless excitations. Still, by increasing the number of sites, the width of this region shrinks, suggesting that this intermediate phase disappears in the thermodynamic limit and the transition

point can be described by the classical Coulomb gas picture.

The paper is organized as follows: In Sec. II, we introduce the variational Jastrow wave function; in Sec. III, we show the numerical results and discuss the mapping to the classical Coulomb gas model, which is pivotal to highlight the physical properties of the Jastrow *Ansatz*; finally, in Sec. IV, we draw our conclusions.

II. THE JASTROW WAVE FUNCTION

Even though the exact ground-state wave function of the Hamiltonian of Eq. (1) is not known on large clusters, its sign structure obeys the so-called Marshall sign rule [28]. Indeed, the model is defined on a bipartite lattice, which can be divided into two sublattices A and B with off-diagonal terms only connecting different sublattices. In addition, the ground state belongs to the sector with zero total magnetization, i.e., $\hat{M} = \sum_j \hat{S}_j^z = 0$. Then, by defining the basis $\{|x\rangle\}$ in which the z component of the spin operator m_j is given on each site (and $M = \sum_j m_j = 0$), the ground state is written as

$$|\Psi_0\rangle = \sum_x (-1)^{N(x)} f(x) |x\rangle, \quad (4)$$

where $f(x) > 0$ is the (unknown) amplitude and $N(x) = \sum_{j \in B} [1 + m_j(x)]$, where $m_j(x)$ is value of \hat{S}_j^z in $|x\rangle$, i.e., $\hat{S}_j^z |x\rangle = m_j(x) |x\rangle$.

The Jastrow wave function is obtained by applying a (positive) Jastrow factor $\hat{\mathcal{J}}$ to a state $|\Phi_0\rangle$ that encodes the Marshall sign rule (within the subspace with $M = 0$):

$$|\Psi_J\rangle = \hat{\mathcal{J}} |\Phi_0\rangle. \quad (5)$$

In our case, we take

$$|\Phi_0\rangle = \hat{\mathcal{P}}_{M=0} \prod_j \frac{1}{\sqrt{3}} [(-1)^j |0\rangle_j + |1\rangle_j + |-1\rangle_j], \quad (6)$$

where $\hat{\mathcal{P}}_{M=0}$ is the projector into the subspace with $M = 0$ and $|0\rangle_j$ and $|\pm 1\rangle_j$ are the eigenkets of \hat{S}_j^z with eigenvalue 0 and ± 1 , respectively. As a result, $|\Phi_0\rangle$ is a linear combination of all possible states with vanishing magnetization and equal weights (the signs of the spin configurations being consistent with the ones of the Marshall-sign rule). We remark that $|\Phi_0\rangle$ resembles the Néel antiferromagnetic state pointing in the x direction, where the local states are given by $1/2[(-1)^j \sqrt{2}|0\rangle_j + |1\rangle_j + |-1\rangle_j]$.

The Jastrow factor has the following form:

$$\hat{\mathcal{J}} = \exp \left\{ \frac{1}{2} \sum_{i,j} v_{i,j} \hat{S}_i^z \hat{S}_j^z \right\}, \quad (7)$$

where $v_{i,j}$ defines the so-called pseudopotential, which, in translationally invariant cases, depends only upon the relative distance between the two sites i and j : $v_{i,j} = v_{|i-j|}$. The correct physical properties are obtained when all the independent distances (e.g., $L/2$ on chains with periodic boundary conditions) are optimized independently.

All physical observables have been computed by standard variational Monte Carlo techniques [1], the error-bars

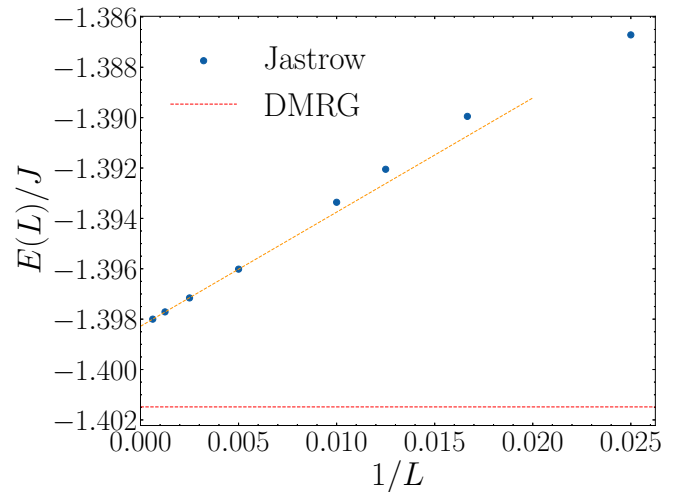


FIG. 1. Energy per site $E(L)/J$ as a function of $1/L$ for the Jastrow *Ansatz* of Eq. (5) with optimized parameters for $D = 0$. The red dashed line corresponds to the thermodynamic value obtained within DMRG, i.e., $E_{\text{DMRG}}/J = -1.401484$, [30] while a linear extrapolation of the energies for the largest sizes gives $E(L \rightarrow \infty)/J = -1.3981(1)$.

being estimated using the binning analysis. The Jastrow pseudopotential is optimized minimizing the variational energy of the $S = 1$ Hamiltonian of Eq. (1) by using the stochastic reconfiguration technique [29]. An excellent approximation can be obtained by a simple parametrization, which includes only two parameters, one for the on-site term and the other one for the long-range behavior (see below). This simplified form of the pseudopotential has a smooth convergence in the thermodynamic limit in Fourier space and is pivotal to give an insightful interpretation of the physical properties. In this case, the two parameters can be easily optimized within standard minimization approaches.

III. RESULTS

Here, we discuss the numerical results obtained by the Jastrow wave function of Eq. (5) for the generalized Heisenberg Hamiltonian of Eq. (1). In addition, we also present the mapping to the classical partition function and the corresponding phase diagram.

A. The Haldane phase at $D = 0$

Let us begin by considering the isotropic Heisenberg point, with $D = 0$, corresponding to the Haldane phase, which is gapped and presents a nonlocal order parameter, see Eq. (3). First, to check how well the Jastrow *Ansatz* is able to reproduce the ground state of the spin-1 Heisenberg model, we compute the variational energy per site $E(L)$ for various sizes and compare it with the thermodynamic extrapolation obtained by the DMRG technique [30], see Fig. 1. For $L = 200$, the relative error is smaller than 0.5% and gets lower when the size of the system increases. By a linear extrapolation of the large-cluster results, we find that the thermodynamic energy of the Jastrow state is $E(L \rightarrow \infty)/J =$

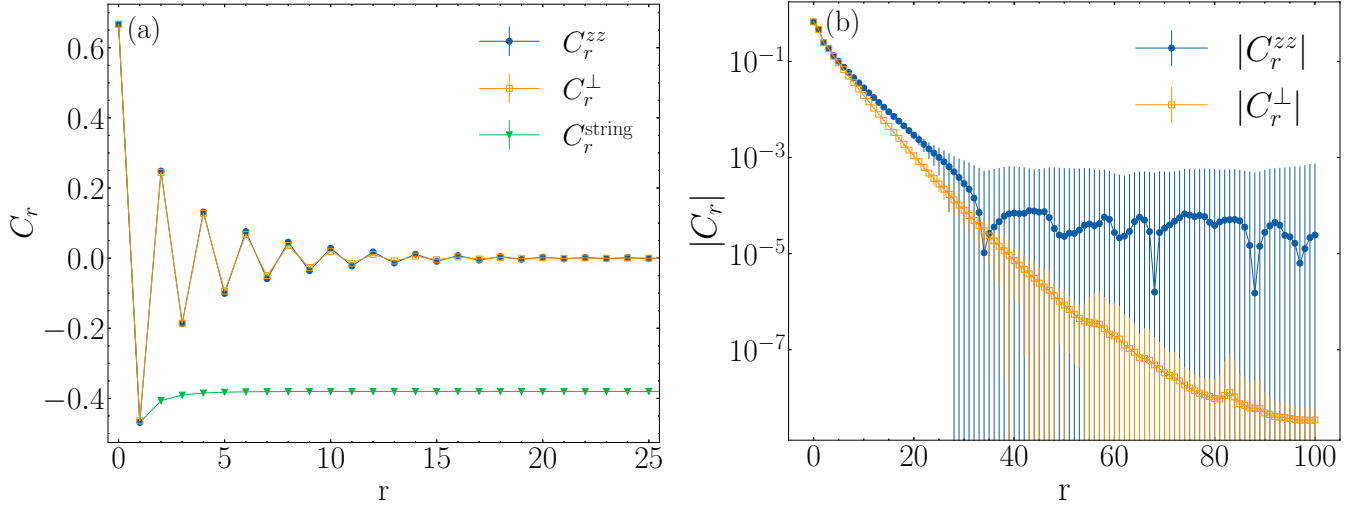


FIG. 2. Correlation functions for the optimized Jastrow state for $D = 0$ and $L = 200$. (a) Spin-spin correlations C_r^{zz} and C_r^\perp and string correlations C_r^{string} [Eqs. (8)–(10)] as a function of r . (b) Absolute value of the correlations C_r^{zz} and C_r^\perp in semilog plot: their behavior is consistent with an exponential decay to zero.

$-1.3981(1)$ (i.e., the relative error with respect to DMRG is about 0.2%).

Remarkably, the Jastrow wave function is able to reproduce the Haldane-phase physics, exhibiting nonvanishing string order and exponentially decaying correlation functions. To show this fact, we report the spin-spin correlation functions,

$$C_r^{zz} \equiv \frac{1}{L} \sum_j \langle \hat{S}_j^z \hat{S}_{j+r}^z \rangle, \quad (8)$$

$$C_r^\perp \equiv \frac{1}{2L} \sum_j \langle (\hat{S}_j^x \hat{S}_{j+r}^x + \hat{S}_j^y \hat{S}_{j+r}^y) \rangle, \quad (9)$$

and the string correlations of the operator of Eq. (2),

$$C_r^{\text{string}} = \frac{1}{L} \sum_j \langle \hat{\sigma}_{j,j+r}^{\text{string}} \rangle. \quad (10)$$

Notice that, since the Jastrow wave function generically breaks the spin $SU(2)$ symmetry, the spin-spin correlations along the z axis and in the x – y plane are different, even though the discrepancy is small. The results for $L = 200$ are reported in Fig. 2. Here, both C_r^{zz} and C_r^\perp are consistent with an exponential decay with distance, while C_r^{string} reaches a constant value, hinting at the presence of string order.

Importantly, the optimized pseudopotential has a long-range tail, which is crucial to reproduce the correct physical behavior of the Haldane phase. In particular, the optimized pseudopotential v_q in Fourier space behaves as $v_q \approx 1/q^2$ for small q , see Fig. 3, where we report $v_q \times q^2$ for various sizes of the chain. The fact that a short-range Jastrow factor is not suitable to describe the Haldane phase is clear by optimizing v_r only for distances $r < r_c$ (i.e., fixing $v_r = 0$ for $r \geq r_c$). In Fig. 4, the results of the x – y spin-spin correlations are reported for $r_c = 10$ on $L = 100$, in comparison to the long-range case with $r_c = 50$. The former case clearly gives a finite value of C_r^\perp for $r \gtrsim r_c$. Furthermore, the string correlations

are suppressed, indicating that no string order is possible whenever the Jastrow factor is not long range.

B. The large D/J limit

We now briefly discuss the regime where $D/J \gg 1$. It turns out that the Jastrow wave function of Eq. (5) also correctly describes this case. Here, the spin-spin correlations are still exponentially decaying with the distance. However, in contrast to the Haldane phase, the string correlations are correctly vanishing for large distance (not shown). Also in this case, the Jastrow pseudopotential v_r has a long-range tail, with $v_q \approx 1/q^2$ in the small- q limit (see Fig. 3), as in the Haldane regime.

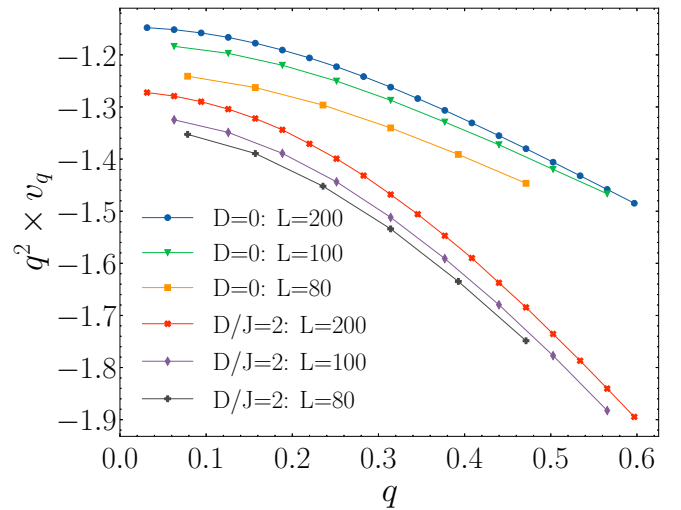


FIG. 3. The optimized Jastrow pseudopotential in Fourier space v_q multiplied by q^2 as a function of q for the Heisenberg model with $D = 0$ and $D/J = 2$ for different values of L . The results show that $v_q \approx 1/q^2$ for $q \rightarrow 0$.

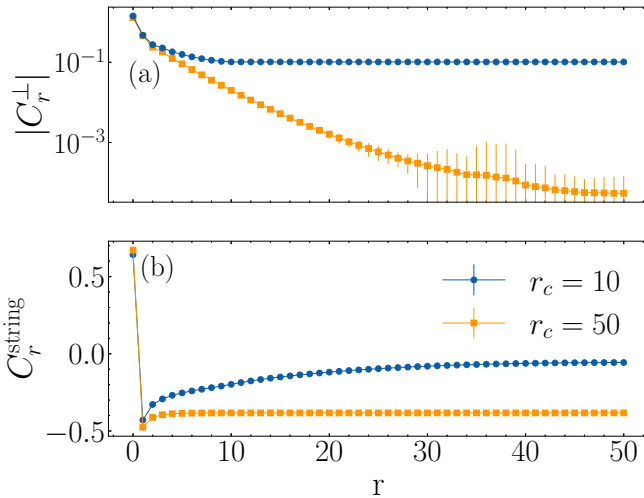


FIG. 4. Correlation functions for the Jastrow factor with a cutoff in the pseudopotential, i.e., $v_r = 0$ for $r > r_c$, compared to the ones with no cutoff. (a) Spin-spin correlations $|C_r^+|$ of Eq. (9). (b) String correlations C_r^{string} of Eq. (10). The case with $r_c = 10$ on $L = 100$ sites is shown for the Heisenberg model with $D = 0$.

The fact that the same kind of behavior in the Jastrow pseudopotential may give rise to both topological (with finite string order parameter) and trivial (with no string order parameter) phases requires a deeper investigation, which is the subject of the next subsection.

C. The classical Coulomb gas mapping

To gain some understanding from the Jastrow wave function, we start by noticing that quantum expectation values over a given variational state can be directly interpreted as thermal expectation values over classical probabilities. The idea underlying the classical mapping is that any quantum average of an operator $\hat{\mathcal{O}}$ over a state $|\Psi\rangle$ can be expressed as a sum over the complete basis set $|x\rangle$,

$$\langle \hat{\mathcal{O}} \rangle = \sum_x \frac{|\langle x|\Psi\rangle|^2}{\langle \Psi|\Psi\rangle} \frac{\langle x|\hat{\mathcal{O}}|\Psi\rangle}{\langle x|\Psi\rangle} = \sum_x P(x) \mathcal{O}(x), \quad (11)$$

such that the wave function (squared) can be interpreted as a classical Boltzmann weight $P(x)$,

$$P(x) = \frac{1}{\mathcal{Z}} e^{-\beta \mathcal{E}(x)}, \quad (12)$$

where $\beta \mathcal{E}(x) = -2 \ln |\langle x|\Psi\rangle|$ defines an effective classical temperature $T = 1/\beta$ and a classical energy $\mathcal{E}(x)$. The quantum expectation value (at zero temperature) is then obtained by averaging the appropriate observable $\mathcal{O}(x)$ over $P(x)$.

In the present scenario, $\langle x|\Psi\rangle$ is fully determined by the Jastrow factor, since $\langle x|\Phi_0\rangle$ of Eq. (6) is constant (apart from the Marshall sign, which is irrelevant because of the modulus squared). The crucial point is that the fully optimized Jastrow pseudopotential $v_{i,j}$ may be accurately approximated by using only two parameters (β and μ),

$$v_{i,j} = \beta \left[\mu \delta_{i,j} - \frac{1}{2L} \left(d_{i,j} - \frac{L}{2} \right)^2 \right], \quad (13)$$

where $d_{i,j} = \min\{|i-j|, L-|i-j|\}$ is the distance between two sites i and j . Therefore, the classical energy $\mathcal{E}(x)$ acquires a particularly simple form in terms of $\{m_1, \dots, m_L\}$ in the configuration $|x\rangle$ (here, for simplicity, we drop the label x in m_j), namely, $\mathcal{E}(x) \rightarrow E(\{m_1, \dots, m_L\})$ with

$$E(\{m_1, \dots, m_L\}) = -\mu \sum_j m_j^2 + \frac{1}{2} \sum_{i,j} U_{i,j} m_i m_j, \quad (14)$$

This expression of the classical energy identifies a one-dimensional lattice gas, where each site may be either empty ($m_j = 0$) or occupied by a unit charge $m_j = \pm 1$. The interaction potential between charges is given by

$$U_{i,j} = \frac{1}{L} \left(d_{i,j} - \frac{L}{2} \right)^2, \quad (15)$$

while the constraint of vanishing total magnetization $\sum_j m_j = 0$ implies charge neutrality, which can be easily enforced by adding a term $\Lambda (\sum_j m_j)^2$ to the classical energy of Eq. (14), with $\Lambda \rightarrow \infty$. This constraint can be enforced by a shift in the interaction potential: $U_{i,j} \rightarrow U_{i,j} + \Lambda$, whose Fourier transform acquires a particularly simple form

$$U_q = \begin{cases} \frac{1}{2[\sin(q/2)]^2} & \text{for } q \neq 0, \\ L\Lambda + \frac{L^2+2}{12} & \text{for } q = 0, \end{cases} \quad (16)$$

which indeed corresponds to a Coulomb-like potential. Thus, the resulting model describes a classical Coulomb gas of particles with charges $q = \pm 1$ in one spatial dimension.

The net consequence of this reasoning is that the quantum expectation values can be rewritten in terms of a classical model, whose partition function is

$$\mathcal{Z} = \sum_{\{m_j\}} e^{-\beta E(\{m_1, \dots, m_L\})}. \quad (17)$$

The physical properties of this classical model are far from being trivial and depend upon the values of the effective temperature $T = 1/\beta$ and of chemical potential μ , which fixes the average number of charges $m_j = \pm 1$. After some straightforward but nontrivial algebra (see Appendix), the partition function can be written in terms of an integral over a continuous variable Q and the trace of a tridiagonal symmetric matrix $\mathbb{T}(Q)$:

$$\mathcal{Z} = \sqrt{\frac{\beta L}{\pi}} \int_{-1/2}^{1/2} dQ \text{Tr} [\mathbb{T}(Q)]^L. \quad (18)$$

The matrix $\mathbb{T}(Q)$ is defined by

$$T_{s,s'}(Q) = t(Q, s, s') [\delta_{s,s'} + e^{\beta\mu} \delta_{s,s'+1} + e^{\beta\mu} \delta_{s,s'-1}],$$

where $t(Q, s, s') = e^{-\frac{\beta}{2} [(Q+s)^2 + (Q+s')^2]}$.

As previously noted [see Eq. (11)], the quantum expectation value (at zero temperature) of an operator $\hat{\mathcal{O}}$ is obtained by averaging the appropriate observable $\mathcal{O}(x)$ over $P(x)$. The matrix elements $\mathcal{O}(x)$ can be easily handled if the corresponding operator $\hat{\mathcal{O}}$ is expressed in terms of the z component of the local spins \hat{S}_j^z . In this case, $\mathcal{O}(x)$ just becomes a function of the classical occupation numbers m_j and the average acquires a transparent meaning, like, for example, the case of

the local density of charges $\langle m_j^2 \rangle$. Following the same procedure detailed in the Appendix, the average density is shown to be given in terms of the above matrix $\mathbb{T}(Q)$ and another matrix $\mathbb{N}(Q)$, with elements $N_{s,s'}(Q) = t(Q, s, s')e^{\beta\mu}[\delta_{s,s'+1} + \delta_{s,s'-1}]$:

$$\langle m_j^2 \rangle = \frac{\int_{-1/2}^{1/2} dQ \text{Tr} \{ \mathbb{N}(Q) [\mathbb{T}(Q)]^{L-1} \}}{\int_{-1/2}^{1/2} dQ \text{Tr} \{ \mathbb{T}(Q) \}^L}. \quad (19)$$

Formally, both $\mathbb{T}(Q)$ and $\mathbb{N}(Q)$ are infinite matrices (s and s' run from $-\infty$ to $+\infty$), but in the thermodynamic limit, two simplifications occur: First, evaluating the trace of $[\mathbb{T}(Q)]^L$ in the basis of the eigenvectors of $\mathbb{T}(Q)$, only the contribution of the eigenvector with the eigenvalue of largest absolute value remains (this is true if the spectrum of $\mathbb{T}(Q)$ is gapped, a condition that is easily checked numerically); in addition, the integral over Q can be evaluated by the steepest descent method and is dominated by the values Q_σ^* maximizing the highest eigenvalue. Therefore, denoting the largest eigenvalue by $\kappa_0(Q)$ (satisfying the relation $\mathbb{T}(Q)|u_0\rangle = \kappa_0(Q)|u_0\rangle$), which is maximized by some values Q_σ^* , the following expressions hold in the thermodynamic limit:

$$\lim_{L \rightarrow \infty} \frac{\ln \mathcal{Z}}{L} = \ln \left[\sum_{\sigma} \kappa_0(Q_\sigma^*) \right], \quad (20)$$

$$\lim_{L \rightarrow \infty} \langle m_j^2 \rangle = \frac{\sum_{\sigma} \langle u_0 | \mathbb{N}(Q_\sigma^*) | u_0 \rangle}{\sum_{\sigma} \kappa_0(Q_\sigma^*)}. \quad (21)$$

Density-density correlations $\langle m_i m_j \rangle$ or string correlations $\langle m_i e^{i\pi \sum_{i+1}^{j-1} m_i} m_j \rangle$ can also be evaluated by relations analogous to Eqs. (19) and (21).

An intuitive picture of the origin of topological order in the one-dimensional Coulomb gas can be gained by noting that the energy of two dipoles in the vacuum does not depend upon the distance between them, being lower for aligned dipoles (e.g., $\{0, 0, +, -, 0, 0, +, -, 0, 0\}$ on $L = 10$) rather than anti-aligned ones (e.g., $\{0, 0, +, -, 0, 0, -, +, 0, 0\}$). As a result, there is a net dipole-dipole attraction, which favors the onset of the string order, identified by the string-order parameter: $\mathcal{S} = \lim_{|i-j| \rightarrow \infty} \langle m_i e^{i\pi \sum_{i+1}^{j-1} m_i} m_j \rangle$.

The zero-temperature properties of the classical Coulomb gas model are easily understood: For $\mu > 1/4$, the lowest-energy configurations are $\{+, -, \dots, +, -\}$ and $\{-, +, \dots, -, +\}$, which correspond to perfect charge-density-wave (Ising antiferromagnetic) states in the charge (spin) language. By contrast, for $\mu < 1/4$ the state $\{0, 0, \dots, 0, 0\}$ has the lowest energy, corresponding to the empty (nematic) state in the charge (spin) language. At finite temperature, the charge-density-wave (antiferromagnetic) order does not survive, instead a state with finite string order emerges, signaling the presence of aligned dipoles in the system. The phase diagram is shown in Fig. 5, displaying two different phases. For $\mu > \mu^*(T)$, there is a (dense) liquid of aligned dipoles, with *finite* string order; instead, for $\mu < \mu^*(T)$ a diluted gas of disordered dipoles, with no string order, stabilizes. In the same figure, we also report the values of the optimal parameters β and μ of the variational wave function with the simplified Jastrow pseudopotential of

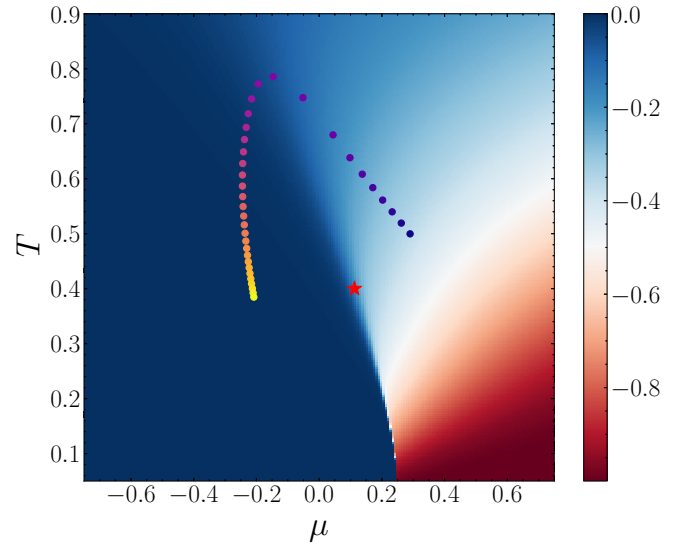


FIG. 5. Phase diagram for the one-dimensional classical Coulomb gas as a function of μ and $T = 1/\beta$ for a system with size $L = 200$. The color map represents the value of the string correlation at the maximum distance; it is easy to recognize the two phases, only the right one displaying string order. The points represented on top of the plot show the optimal parameters β and μ for the variational wave function with the simplified Jastrow pseudopotential, Eq. (13), for a chain of $L = 200$ sites. The values of D/J span from 0 (violet) to 3.4 (yellow). A red star marks the tricritical point where, in the thermodynamic limit, the transition between the phases passes from first order to second order.

Eq. (13), optimized for a chain of $L = 200$ sites and values of D/J ranging from 0 to 3.4. From this picture, we clearly observe the mechanism by which the Jastrow wave function is able to represent both the nematic and topological phases of the Heisenberg chain: while D/J varies, the optimized parameters lead the variational wave function from one phase of the classical model to the other.

The nature of the transition between the two phases may be investigated directly in the thermodynamic limit by inspecting the density and the string parameter. In Fig. 6, we show the average density $\langle m_j^2 \rangle$ and the string order \mathcal{S} as a function of μ for two different values of β . For low temperatures, there is a jump in both the density and string order, indicating that the transition between the dense and diluted phases is first order. In contrast, at higher temperatures, both quantities are continuous, the string-order parameter being zero on the diluted region and finite in the dense one. In this case, a second-order phase transition can be identified. The change from first- to second-order nature is estimated at $\beta \approx 2.5$, as shown in Fig. 6.

D. The ground-state phase diagram of the Heisenberg model

In the previous subsections, we have shown how a simple Jastrow wave function is able to capture the correct physical content both in the topological (Haldane) and large- D (nematic) phases, through a long-range pseudopotential v_r . A simple parametrization gives important insights on the origin of the two phases, with and without string order. Still, the op-

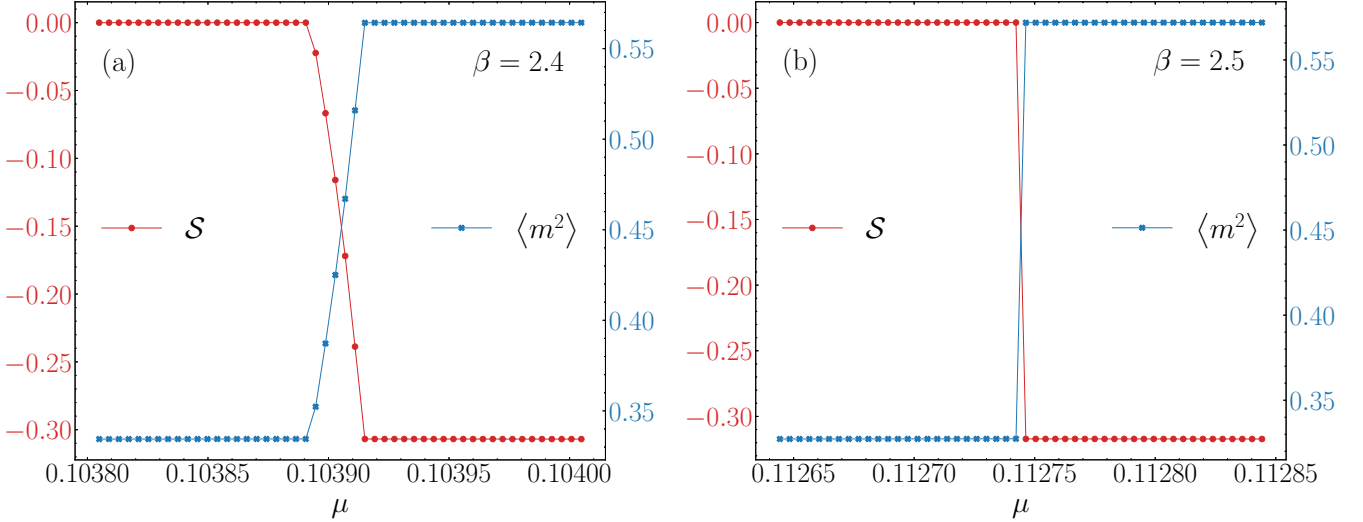


FIG. 6. Density $\langle m^2 \rangle$ and string order \mathcal{S} evaluated in the thermodynamic limit as functions of μ for two different values of β ; in both cases, the scale over which μ varies is very small. (a) For $\beta = 2.4$, the transition between the two phases is second order. (b) For $\beta = 2.5$, the transition is first order.

timal form of v_r deviates from the parametrization of Eq. (13). From a quantitative point of view, an explicit nearest-neighbor term is relevant to improve the variational energy, even well inside the gapped regimes. In Table I, we report the results obtained by using both the optimal Jastrow state and its simplified version, given by the parametrization of Eq. (13).

Most importantly, the simple parametrization does not reproduce the correct small- q behavior of the fully optimized pseudopotential when the transition between topological and large- D phases is approached and the cluster size L is not sufficiently large. Indeed, the transition point is expected to be gapless with power-law correlations [17], which needs a less singular Jastrow factor with $v_q \approx 1/q$ for $q \rightarrow 0$ [22,23]. On small clusters, this kind of pseudopotential is obtained by a full optimization, thus broadening the critical point. Within this intermediate regime, the spin-spin correlations in the x - y plane C_r^\perp show a slow power-law decay, while there are no appreciable string correlations C_r^{string} at large distances. In Fig. 7, we report the results for $C_{L/2}^\perp$ and $C_{L/2}^{\text{string}}$, for different sizes L

TABLE I. Total energies of the simplified (second column) and optimized (third column) Jastrow functions for different values of D/J . The simplified Jastrow pseudo-potential is given by Eq. (13). The relative error is also reported in the fourth column, where $\Delta E = E_{\text{opt}} - E_{\text{simpl}}$. The size of the cluster is $L = 200$.

D/J	E_{simpl}/J	E_{opt}/J	$\Delta E/E_{\text{opt}}$
0.0	-272.11(8)	-279.20(2)	3.64(3) %
0.3	-235.14(7)	-241.36(7)	2.58(4) %
0.5	-212.2(1)	-218.51(9)	2.89(6) %
0.8	-181.08(8)	-188.87(2)	4.12(4) %
1.0	-163.96(7)	-170.89(1)	4.06(4) %
1.5	-130.30(7)	-132.77(3)	1.86(5) %
2.0	-105.04(4)	-105.99(3)	0.90(5) %
2.5	-86.39(3)	-86.76(3)	0.43(5) %
3.0	-72.63(2)	-72.78(2)	0.21(5) %

and values of D/J . Well inside the stable phases, the situation is clear: the Haldane phase has finite $C_{L/2}^{\text{string}}$, while $C_{L/2}^\perp$ vanishes. Instead, for large values of D/J , the nematic phase settles down, where all correlations vanish. In the vicinity of the transition point, for small clusters the in-plane correlations $C_{L/2}^\perp$ are remarkably enhanced. Still, this is a finite-size effect, which disappears when L becomes sufficiently large. Indeed, by increasing the cluster size L , the string-order parameter becomes progressively finite when approaching the transition, while $C_{L/2}^\perp \rightarrow 0$, see Fig. 7. To better quantify this fact, we report in Fig. 8 the area \mathcal{A} below the curve $C_{L/2}^\perp$ in the intermediate phase against $1/L$: this area clearly shrinks to zero in the thermodynamic limit. We mention that a similar effect, with a broadening of the critical behavior is also seen in recent DMRG calculations [31], suggesting that exceedingly

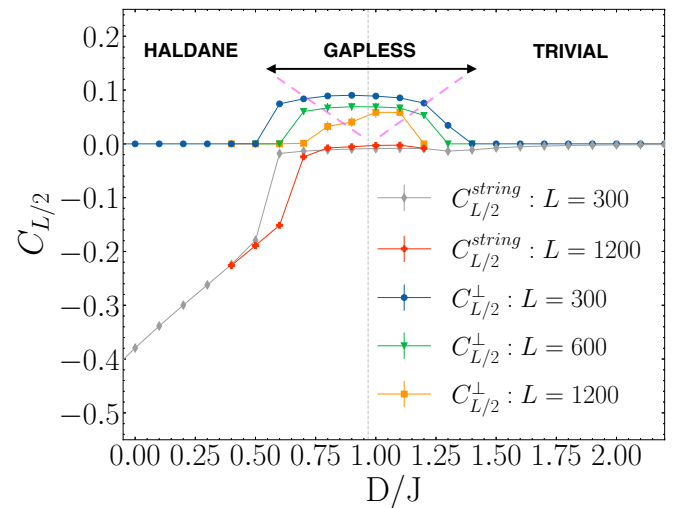


FIG. 7. Order parameters for the Heisenberg chain with single-ion anisotropy D/J , for different sizes L .

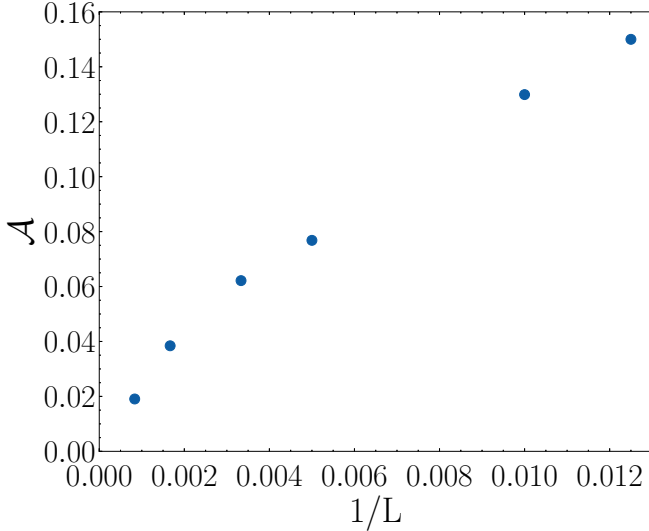


FIG. 8. Area \mathcal{A} enclosed by the curve $C_{L/2}^{\perp}$ for different sizes L plotted against $1/L$. The biggest size we consider is $L = 1200$ and the area is computed from the curve $C_{L/2}^{\perp}$ sampled on a grid of D points with spacing $0.1J$: the area goes to zero in the thermodynamic limit.

large clusters are needed to detect the direct transition between topological and large- D phases.

IV. CONCLUSIONS

In conclusion, we numerically demonstrated that, despite its apparent simple form, the (two-body) Jastrow wave function is able to represent the Haldane phase and describe correctly the phase diagram of a Heisenberg chain with single-ion anisotropy. Therefore, this simple *Ansatz* can reproduce a rich and nontrivial physics, with the advantage of its compactness (it contains only $L/2$ parameters) and its direct physical interpretation. Furthermore, the Jastrow pseudopotential assumes a remarkably simple form, which can be fitted by using a two-parameter function, with an on-site term and a long-range tail. This approximation gives a straightforward interpretation thanks to a mapping between the quantum expectation values over the variational state and a classical partition function. The phase diagram of the latter shows two phases at low temperatures (relevant for the optimized Jastrow pseudopotential): one diluted gas of disordered dipoles (corresponding to the nematic phase of the Heisenberg model with large values of D/J) and one denser liquid of ordered dipoles (corresponding to the Haldane phase). Overall, this paper further highlights the (often overlooked) merits of the Jastrow wave function, which features an optimal balance between accuracy and simplicity also in challenging many-body models.

ACKNOWLEDGMENTS

G.E.S. acknowledges financial support from PNRR MUR Project No. PE000023-NQSTI. G.M. acknowledges financial support from the Swiss National Science Foundation (Grant No. PCEFP2_203455).

APPENDIX: DETAILS FOR THE CLASSICAL PARTITION FUNCTION

Here we provide the formal derivation of the classical partition function given in Eq. (18).

Given a positive definite $L \times L$ matrix \mathbf{A} and a L -dimensional vector \mathbf{m} , the basic identity (Hubbard-Stratonovich transformation) is

$$\int_{-\infty}^{\infty} \prod_j d\phi_j \exp \left\{ - \sum_{j,k} \phi_j A_{j,k} \phi_k + i \sum_j m_j \phi_j \right\} = \sqrt{\frac{\pi^L}{\det \mathbf{A}}} \exp \left\{ - \frac{1}{4} \sum_{j,k} m_j (A^{-1})_{j,k} m_k \right\}. \quad (\text{A1})$$

Then, by taking

$$(A^{-1})_{j,k} = \frac{2\beta}{L} \left[\left(d_{j,k} - \frac{L}{2} \right)^2 + \Lambda L \right], \quad (\text{A2})$$

the partition function is written as

$$\mathcal{Z} = \sqrt{\frac{\det \mathbf{A}}{\pi^L}} \int_{-\infty}^{\infty} \prod_j d\phi_j \exp \left\{ - \sum_{j,k} \phi_j A_{j,k} \phi_k \right\} \times \prod_j \sum_{m=-1,0,+1} e^{\beta \mu m^2 + i m \phi_j}, \quad (\text{A3})$$

where the matrix \mathbf{A} can be easily found because it is diagonalized by Fourier transform,

$$A_{j,k} = \frac{1}{2\beta} \left[\frac{1}{L} \left(\Lambda L + \frac{L^2 + 2}{12} \right)^{-1} + \delta_{j,k} - \frac{1}{2} (\delta_{j,k+1} + \delta_{j,k-1}) \right], \quad (\text{A4})$$

whose determinant is

$$\det \mathbf{A} = \frac{2L^2}{U_0 (4\beta)^L}, \quad (\text{A5})$$

where $U_0 = \Lambda L + \frac{L^2 + 2}{12}$, see Eq. (16). Then, we define

$$\Gamma = \frac{1}{2\beta L U_0}, \quad (\text{A6})$$

such that $\det \mathbf{A} / \Gamma = L^3 / (4\beta)^{L-1}$.

The summation over m in Eq. (A3) can be easily done. Then, by inserting the identity $\int_{-\infty}^{\infty} dx \delta(\sum_j \phi_j - x) = 1$ and using the integral representation of the δ -function $\delta(t) = \int_{-\infty}^{\infty} \frac{d\omega}{2\pi} e^{i\omega t}$, we get

$$\mathcal{Z} = \sqrt{\frac{L^3}{(4\pi\beta)^{L-1}}} \int_{-\infty}^{\infty} \frac{d\omega}{2\pi} e^{-\frac{\omega^2}{4\Gamma}} F(\omega), \quad (\text{A7})$$

where

$$F(\omega) = \int_{-\infty}^{\infty} \prod_j d\phi_j \exp \left\{ - \frac{1}{4\beta} \sum_j (\phi_j - \phi_{j-1})^2 \right\} \times \prod_j e^{i\omega \phi_j} [1 + 2e^{\beta \mu} \cos \phi_j]. \quad (\text{A8})$$

Now, the parameter Λ appears only through Γ ruling the amplitude of the Gaussian term in Eq. (A7). Charge neutrality is enforced when $\Lambda \rightarrow \infty$, i.e., for $\Gamma \rightarrow 0$. The function $F(\omega)$ must have a $\delta(\omega)$ contribution for the partition function to attain a finite limit: If $F(\omega) \approx F_0 \delta(\omega)$ for small ω , the partition function becomes proportional to the amplitude F_0 . Therefore, our main task is the evaluation of the small ω behavior of $F(\omega)$.

The partition function can be written in a more symmetric way by defining the operator [32]:

$$K_\omega(x, x') = \frac{1}{\sqrt{\pi\beta}} \int_{-\infty}^{\infty} dy e^{-\frac{(x-y)^2}{2\beta}} e^{i\omega y} \times [1 + 2e^{\beta\mu} \cos y] e^{-\frac{(y-x')^2}{2\beta}}. \quad (\text{A9})$$

It is easy to check that $F(\omega)$ is just the trace of the product of L of these integral operators,

$$F(\omega) = \int d\phi_1 \dots d\phi_L K_\omega(\phi_1, \phi_2) K_\omega(\phi_2, \phi_3) \dots K_\omega(\phi_L, \phi_1), \quad (\text{A10})$$

which can be also written as

$$F(\omega) = \int d\phi_1 d\phi'_1 \dots d\phi_L d\phi'_L K_\omega(\phi_1, \phi'_1) \times \delta(\phi'_1 - \phi_2) K_\omega(\phi_2, \phi'_2) \delta(\phi'_2 - \phi_3) \dots K_\omega(\phi_L, \phi'_L) \delta(\phi'_L - \phi_1). \quad (\text{A11})$$

By using the integral representation of the δ function

$$\delta(\phi' - \phi) = \int_{-\infty}^{\infty} \frac{dq}{2\pi} e^{iq(\phi' - \phi)}, \quad (\text{A12})$$

the integrals over ϕ and ϕ' can now be performed with the result

$$K_\omega(p, q) = \int d\phi d\phi' e^{-ip\phi + iq\phi'} K_\omega(\phi, \phi') = 4\pi \sqrt{\pi\beta} e^{-\frac{\beta}{2}(q^2 + p^2)} [\delta(q - p + \omega) + e^{\beta\mu} \delta(q - p + \omega + 1) + e^{\beta\mu} \delta(q - p + \omega - 1)]. \quad (\text{A13})$$

In terms of this quantity:

$$F(\omega) = \int \frac{dq_1}{2\pi} \dots \frac{dq_L}{2\pi} K_\omega(q_1, q_2) \dots K_\omega(q_L, q_1). \quad (\text{A14})$$

Due to the specific form of $K_\omega(p, q)$ [see Eq. (A13)], for each choice of q_1 there is a unique choice of q_2 up to q_L and only the integral over q_1 survives. Fixing an arbitrary value of q_1 , the δ functions present in $K_\omega(q_1, q_2)$ force $q_2 = q_1 - \omega + n_2$ with $n_2 = 0, \pm 1$. Then $q_3 = q_1 - 2\omega + n_3$ with $n_3 - n_2 = 0, \pm 1$ and so on. Then all q_j have the form $q_1 - (j - 1)\omega + n_j$ and the last term $K_\omega(q_L, q_1)$ then gives $q_1 = q_L - \omega + (n_{L+1} - n_L)$, i.e., $q_1 = q_1 - L\omega + n_{L+1}$, meaning that $n_{L+1} = 0$ and the function $F(\omega)$ is proportional to a $\delta(L\omega)$. Setting $q_1 = Q + n_1$ with n_1 an arbitrary integer and $|Q| < \frac{1}{2}$, the integral over q_1 splits into an integral over Q and a sum over n_1 , while the condition $n_{L+1} = 0$ implies that $F(\omega)$ is equal to

$$F(\omega) = \sqrt{(4\pi\beta)^L} \delta(\omega L) \int_{-\frac{1}{2}}^{\frac{1}{2}} dQ \text{Tr} [\mathbb{T}(Q)]^L, \quad (\text{A15})$$

which, inserted in Eq. (A7), gives the final expression in Eq. (18).

[1] F. Becca and S. Sorella, *Quantum Monte Carlo Approaches for Correlated Systems* (Cambridge University Press, Cambridge, 2017).

[2] F. Verstraete and J. I. Cirac, [arXiv:cond-mat/0407066](https://arxiv.org/abs/cond-mat/0407066).

[3] D. Perez-Garcia, F. Verstraete, M. M. Wolf, and J. I. Cirac, *Quantum Inf. Comput.* **7**, 401 (2007).

[4] R. Orús, *Nat. Rev. Phys.* **1**, 538 (2019).

[5] G. Carleo and M. Troyer, *Science* **355**, 602 (2017).

[6] G. Torlai, G. Mazzola, J. Carrasquilla, M. Troyer, R. Melko, and G. Carleo, *Nat. Phys.* **14**, 447 (2018).

[7] R. Jastrow, *Phys. Rev.* **98**, 1479 (1955).

[8] W. L. McMillan, *Phys. Rev.* **138**, A442 (1965).

[9] Y. Nomura and M. Imada, *Phys. Rev. X* **11**, 031034 (2021).

[10] N. Astrakhantsev, T. Westerhout, A. Tiwari, K. Choo, A. Chen, M. H. Fischer, G. Carleo, and T. Neupert, *Phys. Rev. X* **11**, 041021 (2021).

[11] F. D. M. Haldane, *Phys. Lett. A* **93**, 464 (1983).

[12] I. Affleck, T. Kennedy, E. H. Lieb, and H. Tasaki, *Phys. Rev. Lett.* **59**, 799 (1987).

[13] T. Kennedy and H. Tasaki, *Phys. Rev. B* **45**, 304 (1992).

[14] F. Pollmann, A. M. Turner, E. Berg, and M. Oshikawa, *Phys. Rev. B* **81**, 064439 (2010).

[15] M. den Nijs and K. Rommelse, *Phys. Rev. B* **40**, 4709 (1989).

[16] W. Chen, K. Hida, and B. C. Sanctuary, *Phys. Rev. B* **67**, 104401 (2003).

[17] S. Hu, B. Normand, X. Wang, and L. Yu, *Phys. Rev. B* **84**, 220402(R) (2011).

[18] A. Langari, F. Pollmann, and M. Siahatgar, *J. Phys.: Condens. Matter* **25**, 406002 (2013).

[19] A. F. Albuquerque, C. J. Hamer, and J. Oitmaa, *Phys. Rev. B* **79**, 054412 (2009).

[20] J.-H. Huang, G.-M. Zhang, and D.-X. Yao, *Phys. Rev. B* **103**, 024403 (2021).

[21] Z.-X. Liu, Y. Zhou, H.-H. Tu, X.-G. Wen, and T.-K. Ng, *Phys. Rev. B* **85**, 195144 (2012).

[22] M. Capello, F. Becca, M. Fabrizio, S. Sorella, and E. Tosatti, *Phys. Rev. Lett.* **94**, 026406 (2005).

[23] M. Capello, F. Becca, M. Fabrizio, and S. Sorella, *Phys. Rev. Lett.* **99**, 056402 (2007).

[24] D. P. Arovas, A. Auerbach, and F. D. M. Haldane, *Phys. Rev. Lett.* **60**, 531 (1988).

[25] R. B. Laughlin, *Phys. Rev. Lett.* **50**, 1395 (1983).

[26] E. Manousakis, *Rev. Mod. Phys.* **63**, 1 (1991).

[27] M. Capello, F. Becca, S. Yunoki, and S. Sorella, *Phys. Rev. B* **73**, 245116 (2006).

[28] W. Marshall, *Proc. R. Soc. Lond. A* **232**, 48 (1955).

[29] S. Sorella, *Phys. Rev. B* **71**, 241103(R) (2005).

[30] S. R. White and D. A. Huse, *Phys. Rev. B* **48**, 3844 (1993).

[31] J. Lambert and E. S. Sørensen, *Phys. Rev. B* **107**, 174427 (2023).

[32] V. Démary, D. S. Dean, T. C. Hammant, R. R. Horgan, and R. Podgornik, *J. Chem. Phys.* **137**, 064901 (2012).